SIAM J. APPL. MATH.
Vol. 70, No. 8, pp. 3086–3104


# FRONTAL REACTION IN A LAYERED POLYMERIZING MEDIUM*

DMITRY GOLOVATY†, L. K. GROSS‡, AND JAMES T. JOYNER†

**Abstract.** We analyze the dynamics of a reaction propagating along a two-dimensional medium of nonuniform composition. We consider the context of a self-sustaining reaction front that converts a monomer-initiator mixture into an inhomogeneous polymeric material. We model the system with one-step effective kinetics, assuming large activation energy. Using asymptotic methods, we find the analytical expressions for the front profile as well as monomer and temperature distributions. Further, we demonstrate that the predictions of the asymptotic theory match well with the numerical simulations.

**Key words.** reaction-diffusion, heterogeneous medium, frontal polymerization, Arrhenius kinetics, asymptotic expansions, ADI method

**AMS subject classifications.** 35K57, 80A30, 80M35, 80M20

**DOI.** 10.1137/100790768

## 1. Introduction.

In this paper we analyze the dynamics of a front propagating along a two-dimensional periodic medium. We determine the impact of the nonuniformity of composition of reagents on interface behavior in the context of frontal polymerization.

Frontal polymerization involves the self-propagation of a reactive zone through an initiator-monomer mixture, rather than simultaneous reaction throughout the mixture. Frontal polymerization can occur via many mechanisms but most frequently through free-radical chain polymerization using initiators, as discussed here.

One can instigate frontal free-radical polymerization by heating a mixture at one end, causing the initiator to decompose into free radicals. The free radicals react exothermically with the monomers. The resulting heat diffuses, causing other initiators to decompose into reactive molecules, perpetuating the polymerization. This interplay between heat generation and heat diffusion causes the front to self-propagate through the mixture, leaving a polymer in its wake. The interface can demonstrate a wide variety of dynamics, depending on problem parameters. Here we consider the regime that supports a wave traveling with constant speed: The heat released during the reaction balances the heat diffused into the mixture of reagents.

Polymerization in the frontal mode requires a mixture with very small reaction rate at ambient temperature but a very rapid rate at the temperature of the front. For sustenance of the front, the high reaction rate must couple with the exothermicity of the reaction to overcome heat losses into the reactant and the product zones. Also the frontal reaction will persist only for sufficiently high ignition temperature.

Liquid monomer can polymerize frontally into a solid product or a very viscous fluid [13]. Adding inactive components such as silica gel to the monomer can reduce flow transport in the system [13]. Here we assume sufficient viscosity of the reagents

*Received by the editors March 31, 2010; accepted for publication (in revised form) August 13, 2010; published electronically November 2, 2010.
http://www.siam.org/journals/siap/70-8/79076.html
†Department of Theoretical and Applied Mathematics, The University of Akron, Akron, OH 44325-4002 (dmitry@uakron.edu, jtjoyner@gmail.com).
‡Department of Mathematics and Computer Science, Bridgewater State University, Bridgewater, MA 02325 (laura.gross@bridgew.edu).

and the final product to eliminate the effects of convection and bubbles from the polymerization dynamics.

A more extensively studied chemical process with a similar reaction mechanism is self-propagating high-temperature synthesis—a combustion process characterized by a heat release large enough to propagate a combustion front through a powder compact while consuming the reactant powders [12]. The simplest models and front-propagation mechanisms for frontal polymerization and self-propagating high-temperature synthesis are essentially the same, except for the magnitudes of the model parameters.

Frontal polymerization was first observed experimentally in the 1970s in the former Soviet Union: Chechilo, Khvilivitskii, and Enikolopyan synthesized polymers under high pressure [7]. Pojman and coworkers have made many recent advances in frontal polymerization experiments [8], [9], dynamics [3], [14], and models [18], [15], [20]. A variety of substances have been synthesized using frontal polymerization, among them polyurethanes [10], polymer films [11], curable unsaturated polyester/styrene resins [11], and functionally gradient materials [8].

Frontal polymerization affords more control over the arrangement of monomers [8], e.g., in a heterogeneous material of which at least one component is a polymer. A nonuniform medium can have desired nonconstant properties, such as a continuously varying refractive index in optical applications. In this study, we characterize the impact of heterogeneity in the fresh mixture on the propagation dynamics and temperature profiles.

We find that small variations of monomer concentration produce leading-order changes in the velocity of the traveling wave. When the front propagates in a system with a discrete number of different initial monomer concentrations, the exact expression for the velocity reduces to a geometric average of velocities corresponding to the concentrations present in the heterogeneous system.

We determine the regions of applicability of the analysis by investigating various parametric regimes. In particular, we show that the temperature is more sensitive to the amplitude of variations of initial monomer concentration than is the front profile.

**2. Model.** Free-radical polymerization includes initiation, propagation, and termination reactions. Five reagents participate: initiator molecules, active initiator radicals, monomer molecules, active polymer radicals, and complete polymer chains [18]. We make several simplifying assumptions that reduce the complexity of the mathematical model. As in [18], [19], [17], consider the following:

- The rates of reactions between the initiator radicals and the monomer and between the polymer radicals and the monomer are the same.
- The rate of change of total radical concentration is much smaller than the rates of their production and consumption.
- The initial concentration of the initiator is so large that it is not appreciably consumed during the polymerization process.
- The material diffusion is negligible compared to the thermal diffusion.

Consider a monomer-initiator mixture occupying $\Omega = \{(x, y) \mid -\infty < x < \infty, 0 < y < L\}$, and denote by $\hat{M}(x, y, t)$ and $\hat{T}(x, y, t)$ the monomer concentration and temperature, respectively, at the point $(x, y) \in \Omega$ and time $t > 0$, where all variables are nondimensionalized as in [6]. Then the free-radical polymerization can be described [17] by what is known as a single-step effective kinetics model of monomer-to-polymer conversion:

$$\hat{M}_t = -K(\hat{T})\hat{M}, \quad \hat{T}_t = \hat{T}_{xx} + \hat{T}_{yy} + K(\hat{T})\hat{M},$$

where

$$K(\hat{T}) = Z \exp\left[\frac{Z(\hat{T}-1)}{\epsilon Z(\hat{T}-1)+1}\right]. \tag{2.1}$$

The effective Zeldovich number $Z$ is a nondimensionalized activation energy [16] constructed (as shown in Table 1 in section 5) as a ratio of the diffusion temperature scale to the reaction temperature scale. The diffusion scale is the difference $T_b - T_i$ between the (dimensional) temperatures of the products and reagents far away from the front. The reaction scale is $\frac{R_g T_b^2}{E}$, where $R_g$ is the universal gas constant, and $E$ is the effective activation energy. Here $\epsilon = \frac{R_g T_b}{E}$, as shown in Table 1. (Note that the table shows values for $Z$ and $\epsilon$ that we use later in simulations.) The definitions of $Z$ and $\epsilon$ imply that $\epsilon Z$ is always less than 1 because $\frac{T_i}{T_b} > 0$.

We impose periodic boundary conditions

$$\hat{T}(x,0,t) = \hat{T}(x,L,t), \quad \hat{T}_y(x,0,t) = \hat{T}_y(x,L,t).$$

The strip $0 < y < L$ can be viewed as a building block for a layered medium.

Far ahead of the front, the monomer distribution is described by

$$\lim_{x\to-\infty} \hat{M}(x,y,t) = 1 + \frac{1}{Z} m(y). \tag{2.2}$$

Figure 1 shows an example of $m(y)$ and illustrates propagation of the front downward in the negative $x$ direction. Although not represented in the sketch in Figure 1, the inhomogeneity in the fresh mixture will produce variation in the final polymer product. Reaction and diffusion effects will also cause the monomer concentration in advance of the front to vary with $x$, as well as to deviate from the initial uniform stripes in $y$ that the figure depicts. In the figure, note that the $x$ interval is truncated from $(-\infty, \infty)$ to a finite interval.

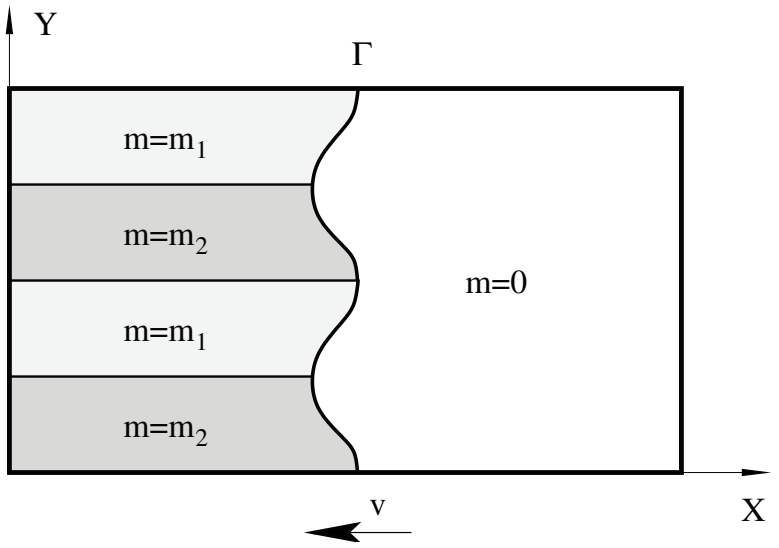


FIG. 1. *Schematic of frontal polymerization in a periodic medium.*

The material is held at a (scaled) temperature of zero far ahead of the reaction:

$$\lim_{x\to-\infty} \hat{T}(x,y,t) = 0.$$

The boundary condition imposed far behind the front is

$$\lim_{x\to\infty} \hat{T}_x(x,y,t) = 0.$$

**3. Traveling-wave solution.** We reexpress the boundary-value problem above in a moving frame by first defining the position of the front $x = \Phi(y,t)$ as the set of points such that

$$\hat{M}(\Phi(y,t),y,t) = \frac{1}{2}. \tag{3.1}$$

A front-attached coordinate $u$ is

$$u = x - \bar{\Phi}(t),$$

where

$$\bar{\Phi}(t) = \frac{1}{L}\int_0^L \Phi(y,t)dy. \tag{3.2}$$

Observe that $u = 0$ represents the average position of the front. ("Averaging" in this work always refers to integration in $y$ from 0 to $L$ and division by $L$.) The dependent variables can be renamed $\hat{M}(x,y,t) = M(u,y,t)$ and $\hat{T}(x,y,t) = T(u,y,t)$.

We consider the reaction wave traveling in the negative $x$ direction with a constant velocity of $v$; that is, $\bar{\Phi}'(t) \equiv v$, where $v$ is a negative constant. Seeking the steady-state solution by setting the time derivatives equal to zero, the system in $M(u,y)$, $T(u,y)$, $v$ (where the front-attached coordinate $u = x - vt$) takes the form

$$-vM_u = -K(T)M, \tag{3.3}$$

$$-vT_u = T_{uu} + T_{yy} + K(T)M, \tag{3.4}$$

subject to periodic boundary conditions in $y$,

$$T(u,0) = T(u,L), \quad T_y(u,0) = T_y(u,L). \tag{3.5}$$

The conditions far ahead of the front are

$$\lim_{u\to-\infty} M = 1 + \frac{1}{Z}m(y), \quad \lim_{u\to-\infty} T = 0. \tag{3.6}$$

The boundary condition imposed far behind the front is

$$\lim_{u\to\infty} T_u = 0. \tag{3.7}$$

Since we are seeking steady-state solutions, the position of the front does not depend on time. Therefore, we denote the position of the front by

$$u = \Phi(y). \tag{3.8}$$

The definition (3.1) of the front position becomes

$$M(\Phi(y), y) = \frac{1}{2}. \tag{3.9}$$

Because of the cold-boundary difficulty [4], the boundary-value problem as written does not have a continuous traveling-wave solution. As such, we modify the kinetics function $K(T)$ to "turn off" far ahead of the front at a prescribed temperature $T_p$ close to zero as follows:

$$K(T) = \begin{cases} 0, & T < T_p, \\ Z \exp\left[\frac{Z(T-1)}{\epsilon Z(T-1)+1}\right], & T \geq T_p. \end{cases} \tag{3.10}$$

**4. Matched asymptotics.** In this section we use matched asymptotic expansions to find a continuous traveling-wave solution $M(u, y)$, $T(u, y)$, and the corresponding constant velocity $v$ in systems with large effective Zeldovich number $Z$, i.e., small

$$\delta = \frac{1}{Z}. \tag{4.1}$$

Because $\epsilon Z$ is sufficiently small, we replace the reaction function (3.10) by

$$K(T) = \begin{cases} 0, & T < T_p, \\ Z \exp[Z(T-1)], & T \geq T_p. \end{cases} \tag{4.2}$$

For the matched asymptotics, we partition the domain into outer reagent and product zones bracketing an inner zone in which most of the reaction takes place. The reaction zone is narrow because the reaction term $ZM \exp[Z(T-1)]$ is significant only at sufficiently high temperatures and monomer concentrations. The method of dominant balance shows that the reaction zone has width $\delta$; we treat the zone as a boundary layer using a stretched coordinate

$$\eta = \frac{u}{\delta} \tag{4.3}$$

there. To distinguish among dependent variables in the three zones, we introduce the notation

$$M(u, y) = M^-(u, y), \quad T(u, y) = T^-(u, y)$$

in the reagent zone,

$$M(u, y) = M^+(u, y), \quad T(u, y) = T^+(u, y)$$

in the product zone, and

$$M(u, y) = M(\delta\eta, y) = \mu(\eta, y), \quad T(u, y) = T(\delta\eta, y) = \tau(\eta, y) \tag{4.4}$$

in the reaction zone.

In each of the three regions, we consider expansions of the corresponding concentration and temperature variables in powers of $\delta$ as follows:

$$F(u, y) = F_0(u, y) + \delta F_1(u, y) + \delta^2 F_2(u, y) + \delta^3 F_3(u, y) + \cdots \tag{4.5}$$

for $F = M^-$, $T^-$ in the reagent zone and $F = M^+$, $T^+$ in the product zone. The dependent variables in the reaction zone expand as

$$g(\eta, y) = g_0(\eta, y) + \delta g_1(\eta, y) + \delta^2 g_2(\eta, y) + \delta^3 g_3(\eta, y) + \cdots, \tag{4.6}$$

where $g = \mu, \tau$. In each zone we substitute the corresponding expansions into the governing partial differential equations (PDEs) and the appropriate boundary conditions from the boundary-value problem (3.3)–(3.7).

To ensure continuity of the monomer and temperature functions at the boundaries between regions, we also impose matching conditions

$$\lim_{u\to 0^-} M^-(u, y) = \lim_{\eta\to-\infty} \mu(\eta, y), \qquad \lim_{\eta\to\infty} \mu(\eta, y) = \lim_{u\to 0^+} M^+(u, y), \tag{4.7}$$

$$\lim_{u\to 0^-} T^-(u, y) = \lim_{\eta\to-\infty} \tau(\eta, y), \qquad \lim_{\eta\to\infty} \tau(\eta, y) = \lim_{u\to 0^+} T^+(u, y). \tag{4.8}$$

Into the matching conditions (4.7)–(4.8), we substitute the expansions (4.5) of the outer variables. We then expand the coefficients $M_i^\pm$, $T_i^\pm$ as Taylor series about $u = 0$ expressed in powers of $\eta$, write $\mu$ and $\tau$ in their asymptotic expansions as in (4.6), and equate like terms to get matching conditions at the various orders of $\delta$.

To find the traveling-wave solution, we solve for terms in the expansions (4.5) of $M^\pm$, $T^\pm$ and terms in the expansions (4.6) of $\mu$ and $\tau$. We do not need to expand the velocity $v$ in order to find all the unknowns to the desired order of accuracy (including $v$ to leading order).

In the reaction zone, the kinetics function (4.2) cannot be exponentially small. It cannot be exponentially large either, as no other term in the equation could balance it. As such, the temperature to leading order there is

$$\tau_0(\eta, y) \equiv 1.$$

Note that it is consistent with the governing equation (3.4) to leading order $\tau_{0\eta\eta} = 0$. In what follows we will match $\tau_0(\eta, y) \equiv 1$ to $T_0^-(u, y)$ as $u$ approaches zero from below and to $T_0^+(u, y)$ as $u$ approaches zero from above.

As in the reaction zone, the source terms cannot be exponentially large in the reagent zone. Rather, the reaction terms are exponentially small ahead of the front. (Note that $T_0^-(u, y) \equiv 1$ would violate the boundary condition in (3.6) that $\lim_{u\to-\infty} T = 0$.) In the reagent zone, the differential equation (3.3) is $-vM_u^- = 0$. Solving it at the various orders of $\delta$ subject to the boundary condition $\lim_{u\to-\infty} M^- = 1 + \delta m(y)$ in (3.6), we get

$$M^-(u, y) = M_0^-(u, y) + \delta M_1^-(u, y) + \delta^2 M_2^-(u, y) + \delta^3 M_3^-(u, y) + \cdots,$$

where

$$M_0^-(u, y) = 1, \quad M_1^-(u, y) = m(y), \quad M_i^-(u, y) = 0, \quad i = 2, 3, \ldots. \tag{4.9}$$

At leading order, the differential equation (3.4) for temperature in the reagent zone is $-vT_{0u}^- = T_{0uu}^- + T_{0yy}^-$, subject to periodic boundary conditions (3.5) in $y$, and $T_0^-$ approaches zero far ahead of the front, per (3.6). The matching condition $\lim_{u\to 0^-} T_0^-(u, y) = \lim_{\eta\to-\infty} \tau_0(\eta, y) = 1$ also holds. The solution to the boundary-value problem is

$$T_0^-(u, y) = e^{-vu}. \tag{4.10}$$

In the product zone, the temperature $T_0^+(u,y) \equiv 1$, which we can show by way of contradiction: Assuming $T_0^+(u,y)$ is not identically equal to 1, the source term is then exponentially small. (It cannot be exponentially large.) If it is exponentially small, then the $O(1)$ problem has solution $T_0^+(u,y) \equiv 1$, which contradicts our assumption. (The $O(1)$ problem in question consists of the differential equation (3.4) at leading order $vT_{0u}^+ = T_{0uu}^+ + T_{0yy}^+$, subject to periodic boundary conditions (3.5) in $y$, and $T_{0u}^+$ approaches zero far behind the front, per (3.7). The matching condition $\lim_{u\to 0^+} T_0^+(u,y) = \lim_{\eta\to\infty} \tau_0(\eta,y) = 1$ also holds.)

With $T_0^+(u,y) \equiv 1$, the source term is present in the product zone, and (3.4) to leading order becomes $M_0^+ \exp(T_1^+) = 0$. Therefore,

$$M_0^+(u,y) \equiv 0.$$

Equation (3.4) to $O(\delta)$ becomes $M_1^+ \exp(T_1^+) = 0$. Therefore,

$$M_1^+(u,y) \equiv 0. \tag{4.11}$$

Later we will see that $M_0^+$, $M_1^+$ satisfy the matching conditions as $u \to 0^+$.

To summarize, we have determined expansions (4.5) in the outer zones to have the forms

$$\begin{aligned} M^-(u,y) &= 1 + \delta m(y), \\ T^-(u,y) &= e^{-vu} + \delta T_1^-(u,y) + \delta^2 T_2^-(u,y) + \cdots, \\ M^+(u,y) &= \delta^2 M_2^+(u,y) + \delta^3 M_3^+(u,y) + \cdots, \qquad (4.12) \\ T^+(u,y) &= 1 + \delta T_1^+(u,y) + \delta^2 T_2^+(u,y) + \cdots, \qquad (4.13) \end{aligned}$$

where $m(y)$ is specified in the boundary condition (3.6). In the inner zone, so far we only know $\tau_0(\eta,y) \equiv 1$ in the expansions (4.6) for $\mu(\eta,y)$ and $\tau(\eta,y)$. Next we determine $\mu_0(\eta,y)$ and $\tau_1(\eta,y)$ in terms of the front position to leading order $\Phi_1(y)$.

To do so, we turn our attention to the governing equations (3.3)–(3.4) transformed into the inner variables and restricted to the relevant order, namely,

$$v\mu_{0\eta} - \mu_0 \exp(\tau_1) = 0, \tag{4.14}$$

$$\tau_{1\eta\eta} + \mu_0 \exp(\tau_1) = 0. \tag{4.15}$$

At the right edge of the inner zone, we have the matching condition

$$\lim_{\eta\to\infty} \mu_0(\eta,y) = \lim_{u\to 0^+} M_0^+(u,y) = 0. \tag{4.16}$$

Another formal matching condition is

$$\lim_{\eta\to-\infty} \tau_1(\eta,y) = \lim_{u\to 0^-} [T_{0u}^-(u,y)\eta + T_1^-(u,y)].$$

Note that it can be expressed as

$$\lim_{\eta\to-\infty} [\tau_1(\eta,y) + v\eta - T_1^-(0,y)] = 0. \tag{4.17}$$

(Here we have applied the definition (4.10) of $T_0^-(u,y)$.) Differentiating condition (4.17) gives the form

$$\lim_{\eta\to-\infty} \tau_{1\eta}(\eta,y) = -v. \tag{4.18}$$

A third matching condition has direct and differentiated forms

$$\lim_{\eta\to\infty}\tau_1(\eta,y)=\lim_{u\to 0^+}[T_{0u}^+(u,y)\eta+T_1^+(u,y)]=T_1^+(0,y), \tag{4.19}$$

$$\lim_{\eta\to\infty}\tau_{1\eta}(\eta,y)=0. \tag{4.20}$$

To derive a tractable PDE, we first add the PDEs (4.14)–(4.15) and integrate from $\eta$ to infinity. Applying boundary conditions (4.16) and (4.20) we get

$$\mu_0=-\frac{1}{v}\tau_{1\eta}, \tag{4.21}$$

which we substitute into the PDE (4.15) for $\mu_0$ to get $\tau_{1\eta\eta}-\frac{1}{v}\tau_{1\eta}e^{\tau_1}=0$. We then integrate from $\eta$ to infinity. This time we apply the boundary condition on $\tau_1$ at infinity in both forms (4.19) and (4.20) to obtain

$$\tau_{1\eta}=\frac{1}{v}\left\{\exp(\tau_1)-\exp[T_1^+(0,y)]\right\}. \tag{4.22}$$

Note that taking the limit as $\eta$ approaches minus infinity and applying the boundary condition with forms (4.17) and (4.18) gives

$$v=-\exp\left(\frac{T_1^+(0,y)}{2}\right). \tag{4.23}$$

Because $v$ is a constant, the equation shows that $T_1^+(0,y)$ is also constant. Using (4.23) to eliminate $T_1^+(0,y)$ in favor of $v$ in (4.22) implies

$$v\tau_{1\eta}=e^{\tau_1}-v^2. \tag{4.24}$$

To solve for $\tau_1$, we first multiply (4.24) by $\exp(\tau_1)$. If we denote

$$U=\exp(\tau_1)$$

(implying $U_\eta=\exp(\tau_1)\tau_{1\eta}$), then we can reexpress equation (4.24) as

$$vU_\eta=U^2-v^2U.$$

Solving by separating the variables $\eta$ and $U$, integrating, substituting $U=\exp(\tau_1)$, and solving for $\tau_1$ gives

$$\tau_1(\eta,y)=\ln\left[\frac{v^2}{1+\beta\exp(v\eta)}\right]. \tag{4.25}$$

Substituting (4.25) for $\tau_1$ into (4.21) for $\mu_0$ gives

$$\mu_0(\eta,y)=1-\frac{1}{1+\beta\exp(v\eta)}. \tag{4.26}$$

In Appendix A we show $\beta$ can be written in terms of the front position to leading order $\Phi_1(y)$ as

$$\beta=\exp[-v\Phi_1(y)]. \tag{4.27}$$

As such, (4.26) and (4.25) can be expressed as

$$\mu_0(\eta, y) = 1 - \frac{1}{1 + \exp\left[-v\Phi_1(y) + v\eta\right]}, \tag{4.28}$$

$$\tau_1(\eta, y) = \ln\left[\frac{v^2}{1 + \exp\left(-v\Phi_1(y) + v\eta\right)}\right]. \tag{4.29}$$

Turning to the product zone, we now state the governing equation (3.4) to the same order as in the reaction zone as $-vT^+_{1u} = T^+_{1uu} + T^+_{1yy}$. We solve the equation by separation of variables, subject to periodic conditions $T(u, 0) = T(u, L)$ and $T_y(u, 0) = T_y(u, L)$, per (3.5). If the solution remains bounded as $u$ approaches infinity, then $T^+_1(u, y)$ is a constant function. We show in Appendix B that $\bar{T}^+_1(u, y)$ approaches $\bar{m}$ as $u$ approaches infinity, where the overbar notation for the average is defined in (3.2) as usual. Therefore,

$$T^+_1(u, y) \equiv \bar{m}. \tag{4.30}$$

We now know the traveling-wave velocity

$$v = -\exp\left(\frac{\bar{m}}{2}\right) \tag{4.31}$$

from (4.30) substituted into (4.23). Observe that the front velocity is the geometric mean of the velocities corresponding to the concentrations present in the heterogeneous system. It is natural to use the average of monomer concentration far ahead of the front to nondimensionalize the concentration. This leads to $\bar{m} = 0$ and $v = -1$—the assumption that we will use from now on.

We now know the temperature to order $\delta$ in the inner and product zones. At order $\delta$, the differential equation (3.4) for temperature in the reagent zone is $-vT^-_{1u} = T^-_{1uu} + T^-_{1yy}$, subject to periodic boundary conditions (3.5) in $y$, and $T^-_1$ approaches zero far ahead of the front, per (3.6). The solution to the linear homogeneous boundary-value problem is

$$T^-_1(u, y) = a_0 e^u + \sum_{n=1}^{\infty} \left\{ a_n \cos\left(\frac{2\pi n y}{L}\right) + b_n \sin\left(\frac{2\pi n y}{L}\right) \right\} \exp\left\{ \frac{1 + \sqrt{1 + \left(\frac{4\pi n}{L}\right)^2}}{2} u \right\}. \tag{4.32}$$

To determine the constants $a_n$ and $b_n$, we apply a matching condition. In particular, the condition (4.17)—now that $\tau_1$ is known per (4.29)—is

$$T^-_1(0, y) = -\Phi_1(y). \tag{4.33}$$

Averaging the expansion (A.1) of $\Phi(y)$ from Appendix A implies $\bar{\Phi}_1 = 0$ (since $\bar{\Phi} = 0$), so we write $\Phi_1(y)$ in the relevant eigenfunction expansion with zero constant term as

$$\Phi_1(y) = \sum_{n=1}^{\infty} \left[ c_n \cos\left(\frac{2\pi n y}{L}\right) + d_n \sin\left(\frac{2\pi n y}{L}\right) \right]. \tag{4.34}$$

Substituting into the condition (4.33) both the series (4.32) for $T^-_1(u, y)$ and the series (4.34) for $\Phi_1(y)$ and equating like terms implies

$$a_0 = 0, \quad a_n = -c_n, \quad b_n = -d_n, \quad n = 1, 2, \ldots. \tag{4.35}$$

Here note that $c_n$ and $d_n$ must be determined in order to know $T_1^-(u,y)$ per (4.32), as well as to know front perturbation $\Phi_1(y)$ per (4.34).

As such, we seek $c_n$ and $d_n$ via a jump condition

$$T_{1u}^+(0,y) - T_{1u}^-(0,y) = \Phi_1(y) - m(y) \tag{4.36}$$

derived in Appendix C. In particular, we substitute into condition (4.36) the definition of $T_{1u}^+(0,y)$ using (4.30) and a series for $T_{1u}^-(0,y)$ using (4.32), where the coefficients have the definitions in (4.35). We also substitute the expansion (4.34) of $\Phi_1(y)$, as well as the eigenfunction expansion

$$m(y) = \sum_{n=1}^{\infty} \left[ f_n \cos\left(\frac{2\pi n y}{L}\right) + g_n \sin\left(\frac{2\pi n y}{L}\right) \right],$$

where the (known) coefficients are

$$f_n = \frac{2}{L}\int_0^L m(y)\cos\left(\frac{2\pi n y}{L}\right) dy, \quad g_n = \frac{2}{L}\int_0^L m(y)\sin\left(\frac{2\pi n y}{L}\right) dy$$

for $n = 1, 2, \ldots$. Equating like terms implies

$$c_n = \frac{-4\int_0^L m(y)\cos\left(\frac{2\pi n y}{L}\right) dy}{L\left[-1+\sqrt{1+\left(\frac{4\pi n}{L}\right)^2}\right]}, \quad d_n = \frac{-4\int_0^L m(y)\sin\left(\frac{2\pi n y}{L}\right) dy}{L\left[-1+\sqrt{1+\left(\frac{4\pi n}{L}\right)^2}\right]}. \tag{4.37}$$

Now $T_1^-(u,y)$ is known via the series (4.32), and front perturbation $\Phi_1(y)$ is known via the series (4.34). Coefficients are defined in (4.35) and (4.37).

To obtain the solution for the temperature to first order, we replace $\eta$ with $Zu$ per (4.1) and (4.3) in the inner solution. To construct the solution along the whole $u$ axis, we add the outer solution to the inner solution and subtract the common part. Then

$$T(u,y) = \begin{cases} e^u + \frac{1}{Z}\left(T_1^- - \ln\left\{\exp\left[\Phi(y) - Zu\right] + 1\right\} + \Phi(y) - Zu\right), & u < 0, \\ 1 - \frac{1}{Z}\ln\left(\exp\left[\Phi(y) - Zu\right] + 1\right), & u \geq 0. \end{cases} \tag{4.38}$$

**5. Comparison with numerical solution.** To verify the asymptotic results of the previous section, we compare them with computations done using an alternating direction implicit (ADI) finite-difference method (see [5]). We simulate the frontal polymerization in a fixed frame until the propagation reaches a constant speed. We present the results in terms of dimensional variables,

$$\begin{bmatrix} \tilde{x} \\ \tilde{y} \end{bmatrix} = \sqrt{\frac{\kappa Z}{k}} \begin{bmatrix} x \\ y \end{bmatrix}, \quad \tilde{t} = \frac{Z}{k}t,$$
$$\tilde{T}(\tilde{x},\tilde{y},\tilde{t}) = T_i + (T_b - T_i)\hat{T}(x,y,t), \quad \tilde{M}(\tilde{x},\tilde{y},\tilde{t}) = M_i\hat{M}(x,y,t),$$

dropping the tildes. Here the parameter $\kappa$ is the thermal diffusivity, and $k$ is the effective preexponential factor for the one-step kinetics (see [19]). $T_i$ is the reagent temperature far ahead of the front, $T_b$ is the reagent temperature plus heat released, and $M_i$ is the leading-order monomer concentration far ahead of the front. The computational domain is $0 \leq y \leq \tilde{L}$, $0 \leq x \leq 40$, where $\tilde{L} = \sqrt{\frac{\kappa Z}{k}}L$. (Below we drop

TABLE 1
*Parameter values.*

| Parameter | Description | Value |
|---|---|---|
| $\epsilon$ | $\frac{R_g T_b}{E}$ | 0.05 |
| $Z$ | $\frac{(T_b - T_i)E}{R_g T_b^2}$ | 7 |
| $\kappa$ | thermal diffusivity | $0.0014\ \frac{\mathrm{cm}^2}{\mathrm{sec}}$ |
| $k$ | effective preexponential factor | $1\ \frac{1}{\mathrm{sec}}$ |
| $T_i$ | reagent temperature far ahead of front | $300\ \mathrm{K}$ |
| $T_b$ | reagent temperature plus heat released | $532.68\ \mathrm{K}$ |
| $M_i$ | average monomer concentration ahead of front | $5.61\ \frac{\mathrm{mol}}{\mathrm{L}}$ |

the tilde from the $\tilde{L}$.) Unless specified otherwise, we use the parameter values listed in Table 1. Note that the choice of $Z$ implies $\delta = 1/7$ per (4.1).

The (dimensionless) temperature $T_p$ in the kinetics function (4.2) is taken to be a small value. The approach is consistent with [1], [2].

Note that condition (2.2) in the dimensional variable $\tilde{M}$ takes the form

$$\lim_{x \to -\infty} M(x, y, t) = M_i + \frac{1}{Z} M_i m(y).$$

In our computations we use

$$m(y) = \begin{cases} M_p, & \frac{L}{4} \le y < \frac{3L}{4}, \\ -M_p, & 0 \le y < \frac{L}{4} \ \text{ or } \ \frac{3L}{4} \le y \le L, \end{cases} \tag{5.1}$$

so

$$\lim_{x \to -\infty} M(x, y, t) = \begin{cases} M_i(1 + \frac{1}{Z} M_p), & \frac{L}{4} \le y < \frac{3L}{4}, \\ M_i(1 - \frac{1}{Z} M_p), & 0 \le y < \frac{L}{4} \ \text{ or } \ \frac{3L}{4} \le y \le L. \end{cases} \tag{5.2}$$

The factor $M_p$ controls the contrast in monomer concentration. In the view of Figure 1, far ahead of the front we have $m_1 = M_p$ and $m_2 = -M_p$. In this section, we take $M_p = 0.25$.

Figure 2 shows the asymptotic position of the front dimensionalized from the eigenfunction expansion (4.34) for $\Phi_1(y)$ and multiplied by $\delta$: $\sqrt{\frac{\kappa Z}{k}} \Phi_1(\sqrt{\frac{k}{\kappa Z}} y)\delta$. We use the first approximately 50 terms and $L = 2$. The figure also shows steady-state numerical results as contour plots for $M(\Phi(y, t), y, t) = \frac{1}{2} M_i$ per (3.1). Note that the asymptotic solution is in the front-attached coordinate system. The numerics ran in a fixed frame until steady state. The figure shows the asymptotic profile appropriately shifted. The curves agree to order $\delta$.

We compared the expression (4.31) for leading-order velocity with the numerical velocity in the case of $m(y)$ as in (5.1) for $M_p = 0.25$. To do so, we ran the numerics to steady state. We then found the slope of the graph of the position of the steadily propagating front versus time, obtaining approximately $-1.0996$. Equation (4.31) gives $v = -1$. The asymptotic and numeric velocities differ by order $\delta$ as they should.

Figure 3 shows the asymptotic and numerical solutions for temperature. Each profile has higher temperatures in the middle strip, which has more monomer initially

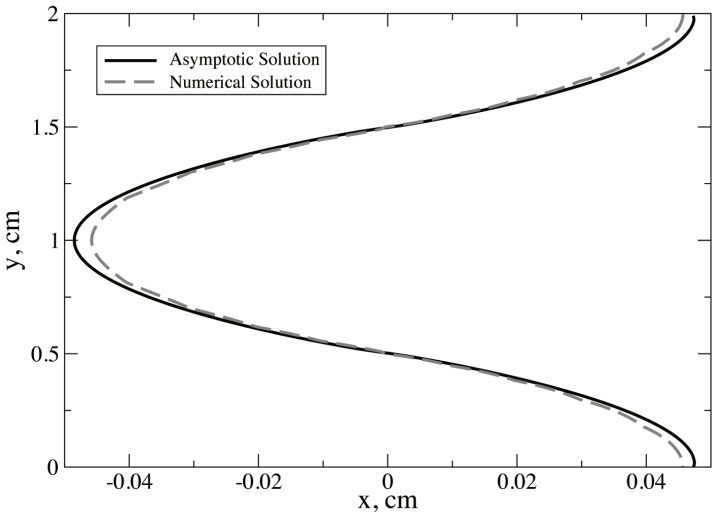


FIG. 2. *The asymptotically and the numerically computed front profiles for* $M_p = 0.25$.

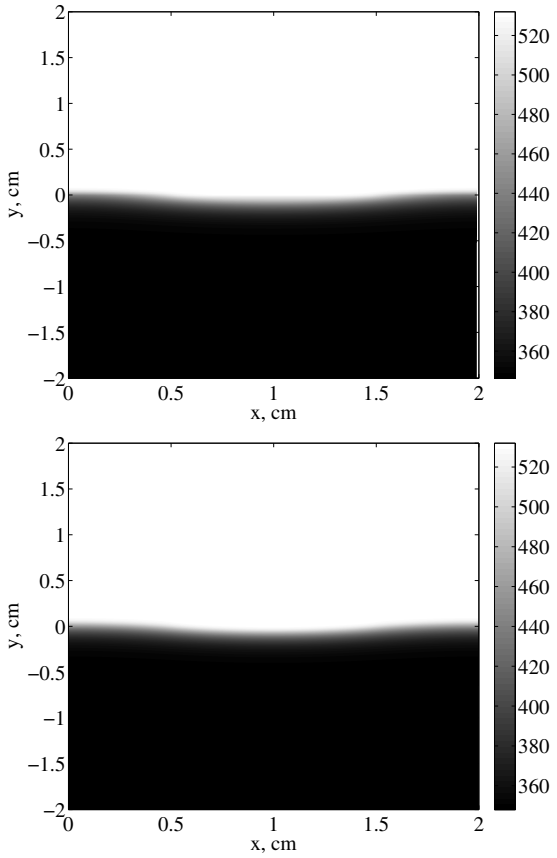


FIG. 3. *The asymptotic solution (top) and the numerical solution (bottom) for the temperature distribution.*

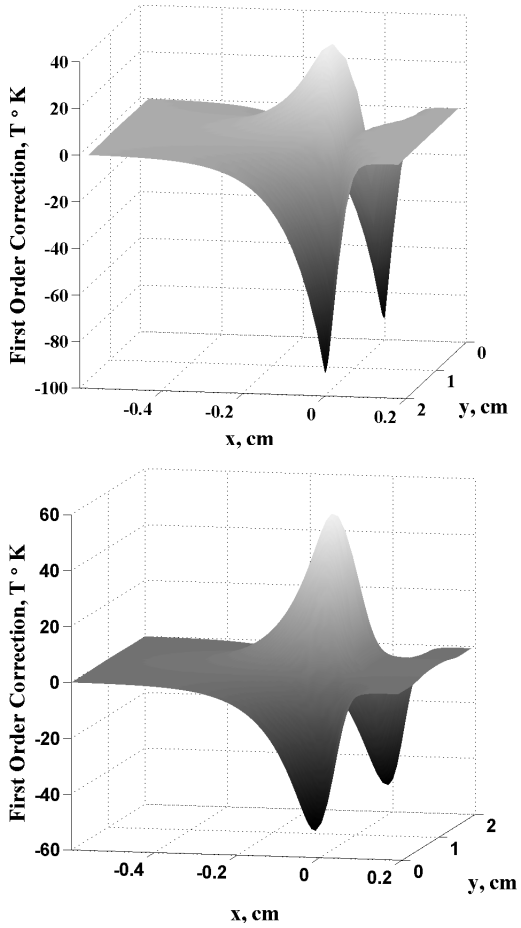


FIG. 4. *The asymptotic solution (top) and the numerical solution (bottom).*

than do the neighboring strips per (5.1). Also the two solutions have mutually consistent temperatures both far behind and far ahead of the front. Note that here we only need a short interval for the numerics to show a steady-state solution.

To show more precisely that the temperatures are close, in Figure 4 we present the first-order corrections for temperature. The top plot shows the order-$\delta$ asymptotic correction to temperature. The bottom plot shows the difference between the numerical solution and the asymptotic leading-order solution. Note that the difference between the corrections when scaled by $T_b - T_i$ is of order $\frac{1}{Z^2}$.

Physically we expect the front profile to deflect more as the monomer perturbation increases. We also expect this trend mathematically because scaling factor $M_p$ in (5.1) enters as a multiplicative constant in the coefficients (4.37) of the terms in the eigenfunction expansion (4.34) of $\Phi_1(y)$. Figure 5 illustrates that the position of the front is sensitive to the amount of variation from the uniform concentration $M_i$ using several $M_p$ values in the boundary condition (5.2).

We demonstrate via Figures 6 and 7 that the asymptotic procedure fails when $M_p$ is sufficiently increased, corresponding to larger perturbations of monomer concentra-

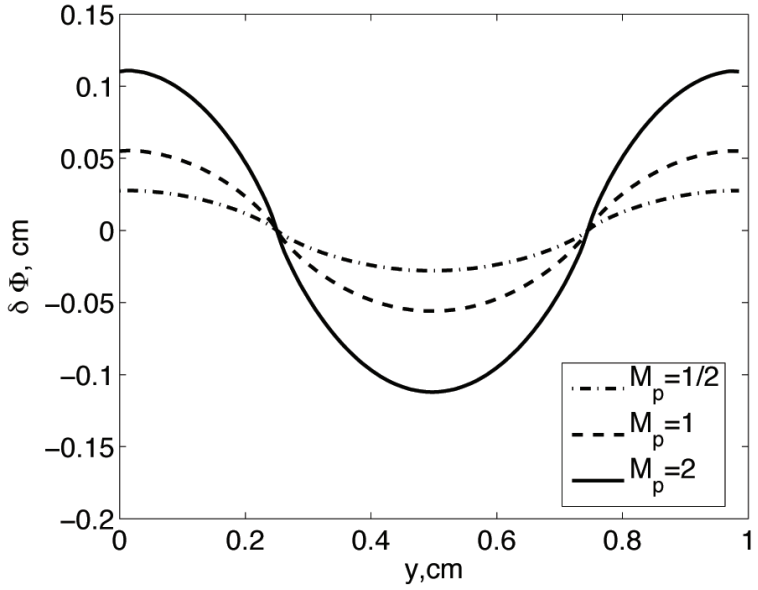


FIG. 5. *The position of the front.*

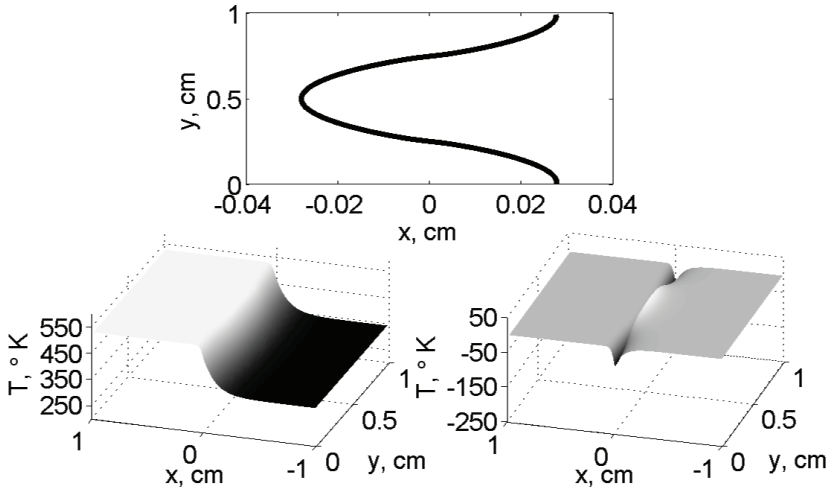


FIG. 6. *The position of the front (top), the leading- and first-order temperature (lower left), and the first-order correction to temperature (lower right) for* $M_p = 0.5$, $\tilde{L} = 1$ *cm, and* $Z = 7$.

tion ahead of the front. Note first that the top graph in each of these figures shows the (dimensionalized) asymptotically determined shape of the front up to the order-$\delta$ term. For Figures 6 (top) and 7 (top), observe that in each of the corresponding regimes ($M_p = 0.5$ and $M_p = 2$, respectively) the front is in fact $O(\delta)$ away from the average position $\bar{\Phi} = 0$.

However, the asymptotic temperature profile is more sensitive to an increase in monomer perturbation than is the front position. In Figures 6 and 7, the lower left plot is the (dimensionalized) asymptotically determined temperature distribution up

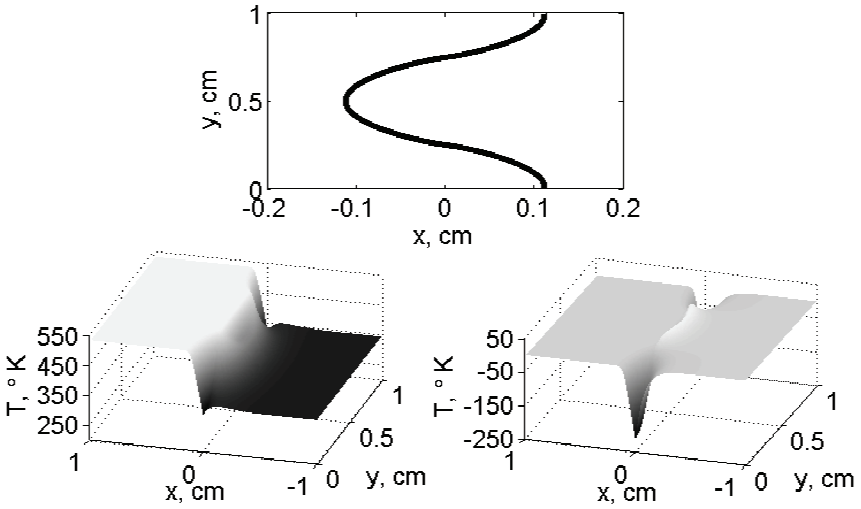


FIG. 7. *The position of the front (top), the leading- and first-order temperature (lower left), and the first-order correction to temperature (lower right) for* $M_p = 2$, $\tilde{L} = 1$ *cm, and* $Z = 7$.

to the order-$\delta$ term. The lower right plot shows the first-order correction to the asymptotic expansion of the temperature. Figure 6 ($M_p = 0.5$) presents a regime of applicability of the asymptotics. In Figure 7 ($M_p = 2$), though, the magnitude of the correction (lower right) is on the order of the leading-order term. The presumed order-$\delta$ correction visibly alters the character of the graph in the lower left. The front position—like the temperature distribution—should not be considered valid, even when the front position happens to coincide with a numerically determined front.

For appropriately small monomer perturbations, the asymptotics fail when the period $L$ becomes too large. Indeed, the denominators for the coefficients in $\Phi_1$ given in (4.37) approach zero as $L \to \infty$. As such, $\Phi_1$ becomes unbounded as $L \to \infty$. An adjustment of our asymptotic analysis is required to handle this situation.

The plots in Figure 8 show the smoothing effect that heat diffusion has on the reaction front when the monomer distributions are discontinuous—as in the cases (5.1) we have already considered here—or highly oscillatory. Such distributions might lead to desirable properties in the polymer, for example, in functionally gradient materials. The asymptotic solution predicts such polymerization features as synthesis time and front behavior.

**6. Conclusions.** We have used the method of matched asymptotic expansions to analyze the propagation of a polymerization front through a heterogeneous monomer-initiator mixture. The front propagates along layers of initial reagents that vary periodically in concentration. The problem setup evokes the polymerization process that produces gradient materials.

We determine leading- and first-order terms for temperature, monomer concentration, front profile, and velocity. We found that the order $1/Z$ variations of monomer concentration lead to order-one changes in the velocity of the traveling wave. When the front propagates in a system with a discrete number of different initial monomer concentrations, the exact expression for the velocity reduces to a geometric average of velocities corresponding to the concentrations present in the heterogeneous system.

We determine the regions of applicability of the analysis by investigating various

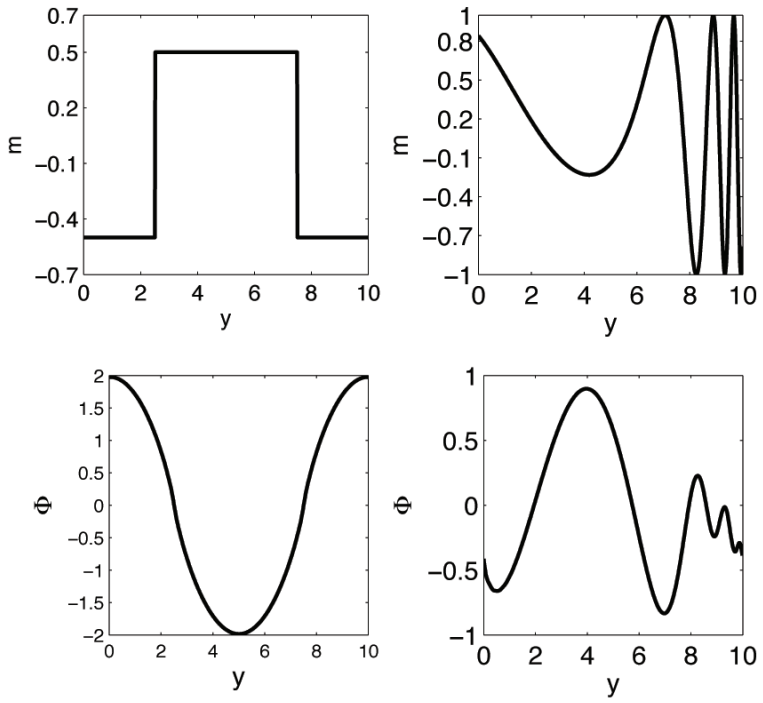


FIG. 8. *The position of the (nondimensional) front (lower left) with the discontinuous monomer distribution from* (5.1) *(top left) and the position of the front (lower right) with a highly oscillatory monomer distribution (top right). Here* $L = 10$.

parametric regimes. In particular, we show that the temperature is more sensitive to the amplitude of variations of initial monomer concentration than is the front profile.

Further, the heat diffusion has a "smoothing" influence on the monomer profile for the parameter values that we consider. In particular, the derivative of the front position function is continuous across the boundary between the regions with two distinct monomer concentrations.

**Appendix A.** To derive $\beta = \exp[-v\Phi_1(y)]$ as in (4.27), first we expand the steady-state front position $\Phi(y)$ of (3.8) in terms of the small parameter $\delta$. Since we assumed that variations of the interface are of order $\delta$ and $\bar{\Phi}$ is zero, $\Phi(y)$ has the form

$$\Phi(y) = \delta\Phi_1(y) + \delta^2\Phi_2(y) + \cdots . \tag{A.1}$$

Substituting the expansion (A.1) of the front position $\Phi(y)$ into the front definition (3.9) gives

$$M(\delta\Phi_1(y) + \delta^2\Phi_2(y) + \cdots, y) = \frac{1}{2}.$$

Expanding the left-hand side in a Taylor series gives

$$M(\delta\Phi_1(y), y) + \cdots = \frac{1}{2}.$$

We rewrite the equation as

$$\mu(\Phi_1(y), y) + \cdots = \frac{1}{2}$$

by making a change of variables in (4.4). Expanding $\mu$ in powers of $\delta$ per (4.6) gives the leading-order equation

$$\mu_0(\Phi_1(y), y) = \frac{1}{2}.$$

Substituting the expression for $\mu_0(\eta, y)$ from (4.26) into the equation above leads to the desired expression $\beta = \exp[-v\Phi_1(y)]$ as in (4.27).

**Appendix B.** Here we derive the condition

$$\lim_{u\to\infty} \bar{T}_1^+(u, y) = \bar{m}. \tag{B.1}$$

First, adding the PDEs (3.3)–(3.4) yields

$$-v(M + T)_u = T_{uu} + T_{yy}.$$

Averaging the equation and applying the periodic boundary conditions (3.5) in $y$ gives

$$-v(\bar{M} + \bar{T})_u = \bar{T}_{uu},$$

where the overbar notation is defined in (3.2) as usual. Integrating along the whole $u$ axis yields

$$-v\left[\lim_{u\to\infty}(\bar{M} + \bar{T}) - 1 - \delta\bar{m}\right] = 0. \tag{B.2}$$

Here we have applied the averages of each of the conditions in (3.6)–(3.7) on $M$ and $T$ at plus and minus infinity, assuming $T$ decays to zero far ahead of the front. (Recall $1/Z = \delta$, per (4.1).)

As $u$ approaches infinity, we expand $M$ and $T$ as $M^+$ and $T^+$, respectively, in powers of $\delta$ per (4.12)–(4.13). In averaged form, the expansions we substitute into (B.2) are

$$\bar{M}(u) = \bar{M}^+(u) = \delta^2\bar{M}_2^+(u) + \cdots,$$
$$\bar{T}(u) = \bar{T}^+(u) = 1 + \delta\bar{T}_1^+(u) + \delta^2\bar{T}_2^+(u) + \cdots.$$

We conclude that (B.1) holds, as desired.

**Appendix C.** To derive a jump condition that will prove useful in determining the order-$\delta$ temperature in the fresh mixture, note that the order-$\delta$ problem in the reaction zone is

$$v\mu_{1\eta} - \mu_1\exp(\tau_1) - \mu_0\exp(\tau_1)\tau_2 = 0, \tag{C.1}$$
$$\tau_{2\eta\eta} + \mu_1\exp(\tau_1) + \mu_0\exp(\tau_1)\tau_2 = -v\tau_{1\eta}. \tag{C.2}$$

At the left edge of the inner zone, we have the matching condition

$$\lim_{\eta\to-\infty} \mu_1(\eta, y) = m(y). \tag{C.3}$$

Another formal matching condition is

$$\lim_{\eta\to-\infty}\tau_2(\eta,y)=\lim_{u\to0^-}\left[\frac{T^-_{0uu}(u,y)}{2}\eta^2+T^-_{1u}(u,y)\eta+T^-_2(u,y)\right].$$

It can be expressed as

$$\lim_{\eta\to-\infty}\left[\tau_2(\eta,y)-\frac{v^2}{2}\eta^2-T^-_{1u}(0,y)\eta-T^-_2(0,y)\right]=0. \tag{C.4}$$

(Here we have applied the definition (4.10) of $T^-_0(u,y)$.) Differentiating condition (C.4) gives the form

$$\lim_{\eta\to-\infty}[\tau_{2\eta}(\eta,y)-v^2\eta-T^-_{1u}(0,y)]=0. \tag{C.5}$$

A formal matching condition at the right edge of the inner zone is

$$\lim_{\eta\to\infty}\tau_2(\eta,y)=\lim_{u\to0^+}\left[T^+_{1u}(u,y)\eta+T^+_2(u,y)\right].$$

Note that it can be expressed as

$$\lim_{\eta\to\infty}\left[\tau_2(\eta,y)-T^+_{1u}(0,y)\eta-T^+_2(0,y)\right]=0. \tag{C.6}$$

(Here we have applied the definition (4.10) of $T^-_0(u,y)$.) Differentiating condition (C.6) gives the form

$$\lim_{\eta\to\infty}\tau_{2\eta}(\eta,y)=T^+_{1u}(0,y). \tag{C.7}$$

Adding the differential equations (C.1), (C.2), integrating along the whole $\eta$ axis, applying conditions (C.3)–(C.7), and setting $v$ to $-1$, we get the jump condition (4.36), as desired.

## REFERENCES


[1] A. Bayliss and B. Matkowsky, *Fronts, relaxation oscillations, and period doubling in solid fuel combustion*, J. Comput. Phys., 71 (1987), pp. 147–168.

[2] A. Bayliss and B. J. Matkowsky, *Two routes to chaos in condensed phase combustion*, SIAM J. Appl. Math., 50 (1990), pp. 437–459.

[3] M. Bazile, Jr., H. Nichols, J. Pojman, and V. Volpert, *Effect of orientation on thermoset frontal polymerization*, J. Polym. Sci. Part A Polym. Chem., 40 (2002), pp. 3504–3508.

[4] H. Berestycki, B. Larrouturou, and J. M. Roquejoffre, *Mathematical investigation of the cold boundary difficulty in flame propagation theory*, in Dynamical Issues in Combustion Theory, IMA Vol. Math. Appl. 35, Springer, New York, 1991, pp. 37–61.

[5] S. Cardarelli, *A Finite-Difference Method to Solve a Frontal Polymerization Model in a 2-Dimensional Rectangular Domain*, unpublished manuscript, University of Akron, 2005.

[6] S. A. Cardarelli, D. Golovaty, L. K. Gross, V. T. Gyrya, and J. Zhu, *A numerical study of one-step models of polymerization: Frontal vs. bulk mode*, Phys. D, 206 (2005), pp. 145–165.

[7] N. Chechilo, R. Khvilivitskii, and N. Enikolopyan, *On the phenomenon of polymerization reaction spreading*, Dokl. Akad. Nauk SSSR, 204 (1972), pp. 1180–1181.

[8] Y. Chekanov and J. Pojman, *Preparation of functionally gradient materials via frontal polymerization*, J. Appl. Polym. Sci., 78 (2000), pp. 2398–2404.

[9] A. Khan and J. Pojman, *The use of frontal polymerization in polymer synthesis*, Trends Polym. Sci., 4 (1996), pp. 253–257.

[10] A. Mariani, S. Bidali, S. Fiori, G. Malucelli, and L. Ricco, *New vistas in frontal polymerization*, Macromolecular Symposium, 218 (2004), pp. 1–9.
[11] A. Mariani and S. Fiori, *Recent developments in frontal polymerization*, Polymer Preprints, 43 (2002), pp. 814–815.
[12] A. G. Merzhanov, A. K. Filonenko, and I. P. Borovinskaya, *New phenomena in combustion of condensed systems*, Dokl. Akad. Nauk USSR (Soviet Phys. Dokl.), 208 (1973), pp. 122–125 (892–894).
[13] M. Perry, V. Volpert, L. L. Lewis, H. A. Nicols, and J. A. Pojman, *Free-radical frontal copolymerization: The dependence of the front velocity on the monomer feed composition and reactivity ratios*, Macromolecular Theory Simul., 12 (2003), pp. 276–286.
[14] J. Pojman, R. Craven, A. Khan, and W. West, *Convective instabilities in traveling fronts of addition polymerization*, J. Phys. Chem., 96 (1992), pp. 7466–7472.
[15] J. A. Pojman, V. Viner, B. Binici, S. Lavergne, M. Winsper, D. Golovaty, and L. K. Gross, *Snell's law of refraction observed in thermal frontal polymerization*, Chaos, 17 (2007), article 033125.
[16] D. A. Schult, *Matched asymptotic expansions and the closure problem for combustion waves*, SIAM J. Appl. Math., 60 (1999), pp. 136–155.
[17] D. A. Schult and V. A. Volpert, *Linear stability analysis of thermal free radical polymerization waves*, Internat. J. Self-Propagating High-Temperature Synthesis, 8 (1999), pp. 417–440.
[18] S. Solovyov, V. Ilyashenko, and J. Pojman, *Numerical modeling of self-propagating polymerization fronts: The role of kinetics on front stability*, Chaos, 7 (1997), pp. 331–340.
[19] C. Spade and V. Volpert, *On the steady state approximation in a thermal free radical frontal polymerization*, Chem. Engrg. Sci., 55 (2000), pp. 641–654.
[20] V. G. Viner, J. A. Pojman, and D. Golovaty, *The effect of phase change materials on the frontal polymerization of a triacrylate*, Phys. D, 239 (2010), pp. 838–847.